



Cite this: RSC Adv., 2017, 7, 34170

## Time-dependent responses of earthworms to soil contaminated with low levels of lead as detected using $^1\text{H}$ NMR metabolomics<sup>†</sup>

 Ronggui Tang,<sup>ad</sup> Changfeng Ding,<sup>a</sup> Yibing Ma,<sup>b</sup> Junsong Wang,<sup>c</sup> Taolin Zhang<sup>a</sup> and Xingxiang Wang<sup>ID \*a</sup>

$^1\text{H}$  NMR-based metabolomics was used to profile the time-dependent metabolic responses of earthworms (*Eisenia fetida*) that were exposed to low-Pb-contaminated-soil (L-Pb-CS) for 28 days using an indoor culture. Earthworms were gathered after days 1, 7, 14, 21 and 28 of the exposure. The earthworm extracts were then analyzed using 500 MHz nuclear magnetic resonance. Spectrum interpretation, statistical analysis and plotting were performed using the "R" software. The metabolic trajectories, histopathological examination, Pb accumulation, survival rate and mean weights of the earthworms were evaluated to investigate and explain the possible mechanism of action. The results showed that the Pb concentrations of earthworms in the Pb exposure groups increased with longer exposure times. Pb treated groups showed varying degrees of histopathological damage. The metabolic response trajectories in the Pb treated groups were of a similar type but differed in the magnitudes of metabolite responses, which suggested that the responses of the Pb1 and Pb2 groups may involve the same metabolic mechanism. Earthworms may produce a toxic response on days 1–14, whereas a detoxification strategy was initiated during days 14–28 to adapt to the L-Pb-CS, as indicated by the negative maximum distance of metabolic trajectories. Specifically, the most serious damage in the histopathology examination and the most extreme values of metabolites were observed on the 14<sup>th</sup> day. The metabolic changes involved the amino acid, membrane, and energy metabolism of earthworms. Myo-inositol, 2-hexyl-5-ethyl-3-furansulfonate (HEFS), scyllo-inositol, succinate, alanine and maltose were found to be potential biomarkers for exposure to the L-Pb-CS. This study demonstrated that  $^1\text{H}$  NMR-based metabolomics along with metal accumulation and histological detection provide a reliable approach for interpreting time-dependent metabolic mechanisms in earthworms.

Received 19th April 2017

Accepted 1st July 2017

DOI: 10.1039/c7ra04393g

[rsc.li/rsc-advances](http://rsc.li/rsc-advances)

### 1. Introduction

Metabolomics is the study of low molecular weight compounds within cells and tissues and how their composition varies in response to an external stressor.<sup>1</sup> Recently, metabolomics has been used as an emerging study approach in numerous fields such as toxicology, drug discovery and environmental stress.<sup>2–4</sup> Environmental metabolomics is

a branch of metabolomics that characterizes the metabolite profiles of organisms and their interactions with the environment.<sup>5</sup> Although environmental metabolomics allows an in-depth investigation into the interactions between organisms and the environment and provides insights into an organism's health at a molecular level,<sup>3</sup> it is currently in its infancy in terms of application in Soil Science. Earthworms, which are ubiquitous species that are in direct contact with the soil system, are easy to sample and identify. For these reasons, they are often used as a model organism to monitor contaminated soil toxicity.<sup>6</sup> *Eisenia fetida* (*E. fetida*) earthworms are often used as model organisms in the eco-toxicological studies according to the recommendation of the Organization for Economic Co-operation and Development (OECD).<sup>7</sup> In past years, high-frequency nuclear magnetic resonance ( $^1\text{H}$  NMR) metabolomics which permits the simultaneous measurement of numerous endogenous metabolites has become popular as a tool for the characterization of earthworm responses to various pollutants. This approach has identified some possible biomarkers such as alanine.<sup>8–10</sup> The metabolic responses of

<sup>a</sup>Key Laboratory of Soil Environment and Pollution Remediation, Institute of Soil Science, Chinese Academy of Sciences, Nanjing, 210008, People's Republic of China.  
E-mail: xxwang@issas.ac.cn; Tel: +86-02586881200

<sup>b</sup>Institute of Agricultural Resources and Regional Planning, Chinese Academy of Agricultural Sciences, Beijing, 100081, People's Republic of China

<sup>c</sup>Center for Molecular Metabolism, School of Environmental and Biological Engineering, Nanjing University of Science and Technology, Nanjing, 210014, People's Republic of China

<sup>d</sup>University of the Chinese Academy of Sciences, Beijing, 100049, People's Republic of China

† Electronic supplementary information (ESI) available. See DOI: 10.1039/c7ra04393g



earthworms to a lead nitrate solution has been investigated using a filter paper contact test.

Furthermore, metabolomics is also concerned with characterizing the time-dependent metabolic responses of living organisms to physiological perturbations.<sup>1,4</sup> The metabolic responses as functions of the exposure time have provided valuable information in terms of the mechanism of action (MOA) of organic contaminants in organisms.<sup>11–13</sup> Further, building time-dependent relationships between the metabolite changes and pollutants exposure is critical for ecotoxicological assessments of pollutants that use a NMR-based earthworm metabolomics approach such as organic pollutants.<sup>14</sup>

According to the OECD guideline, the mortality, mean weight and cocoon production are generally used as endpoints for assessments of toxicity in earthworms.<sup>7</sup> However, these parameters may not change significantly during experiments that involve the short-term exposure to soils with low levels of contamination. In China, Pb contaminated arable soil, in which moderate and low concentrations of this pollutant predominate, is a serious issue.<sup>15</sup> Furthermore, given the increasing concern about heavy metal pollution in the soil, it will be helpful for the public and policy makers to know the potential toxic effects of the low-Pb-contaminated-soil (L-Pb-CS, environmentally relevant concentrations). In addition, clarifying the time-dependence of the toxic mechanism in the L-Pb-CS will be of great practical significance, by providing early screening for warning biomarkers of lead pollutants that may lead to adverse chronic effects in the soil environment. However, the relationships between the toxic effects of the L-Pb-CS to earthworms and the time-dependent effects of the exposure have seldom been reported. Therefore, a more sensitive method such as metabolomics is needed to develop an assessment of the possible time-dependent toxic effects of L-Pb-CS.

Our first objective was to confirm whether <sup>1</sup>H NMR-based metabolomics was able to detect the time-dependent metabolic changes even induced by L-Pb-CS; second, to determine which kinds of metabolites in earthworms were influenced by L-Pb-CS and find possible biomarkers; and finally, to evaluate the potentially different response mechanisms during different exposure stages.

## 2. Methods and materials

### 2.1 Soil preparation

In the present study, ferrosol (F) derived from quaternary red clay was gathered from the Ecological Experimental Station of Red Soil, Chinese Academy of Sciences, Yingtan City, China. The relevant parameters of the ferrosol are presented in Table S1.<sup>†</sup> On the basis of the Pb limit for the second grade of soil (the highest soil Pb concentration allowable for crop production) of the National Soil Environmental Quality Standard of China (NSEQSC, GB 15618-1995), 125 and 250 mg kg<sup>-1</sup> of a Pb(NO<sub>3</sub>)<sub>2</sub> solution, which are one half and one times the limit, respectively, were added to the ferrosol, respectively. These exposure mediums were considered soils with low levels of contamination soils on the basis that the degree of soil contamination designated low, medium, or severe when the concentration is 1–

3, 3–5, or >5 times the benchmark value, respectively.<sup>16</sup> Three months later, the ferrosol was used to plant root vegetables. Five years later, the contaminated ferrosol was milled and sieved to 2 mm. The Pb concentrations in the three treated ferrosol samples (control, Pb1 and Pb2) were determined to be 23.2, 133.2 and 248.7 mg kg<sup>-1</sup>. Then 500 g of ferrosol was transferred into a 1 L breaker and adjusted to 35% moisture content of the soil dry weight using deionized water. A total of 45 beakers were utilized to conduct the experiments (Fig. S1†).

### 2.2 Earthworm exposure

To allow acclimation to the laboratory conditions, *E. fetida* earthworms that were purchased from a worm farmland in Jurong city, Jiangsu province, China were raised in an incubator for four weeks. Mature earthworms, as indicated by a visible clitellum (400–600 mg), were selected to conduct the experiment. After two days of depuration, ten earthworms were added to each of three replicate beakers, which were filled with Pb contaminated or control ferrosol. All beakers were covered with gauze to prevent the earthworms from escaping. A total of 450 earthworms were used to carry out the experiment. On the 0<sup>th</sup>, 7<sup>th</sup>, 14<sup>th</sup> and 21<sup>st</sup> days, 5 g of cattle manure was placed on the surface of the exposed soils as the food of earthworms. According to the OECD's guidelines, the earthworms were kept in a closed incubator at 20 ± 1 °C, with 80% humidity and a light intensity of 600 lux.<sup>7</sup>

### 2.3 Analysis of Pb concentrations in the earthworms

Three earthworms (*n* = 3) were selected from the replicates of each treated group on the 1<sup>st</sup>, 7<sup>th</sup>, 14<sup>th</sup>, 21<sup>st</sup> and 28<sup>th</sup> days. After voiding the gut contents for 4 days on wet filter, the earthworms were rinsed, flash-frozen, lyophilized and weighed. Each earthworm sample (0.08–0.12 g) was then digested independently for 4 hours at 140 °C in a mixture of 5 mL of 65–68% HNO<sub>3</sub> and 3 mL 30% of H<sub>2</sub>O<sub>2</sub> (guaranteed reagent). After that, the digests were diluted appropriately with ultrapure water and then analyzed using inductively coupled plasma mass spectrometry (ICP-MS). The recovery rate for the standard substance (GBW10049, Green Chinese onion, National Quality and Technology Supervision Agency of China) was 98.5–101.7%, and the coefficient of variation (CV) was below 5%.

### 2.4 Histological examinations of the earthworms

Three earthworms (*n* = 3) in each treated groups were cut transversely into three parts and fixed in 4% buffered paraformaldehyde for 24 h. After processing, wax-embedded sections (5 µm) were cut, stained with hematoxylin and eosin, and examined using light microscopy.

### 2.5 Solvent extractions of earthworm tissues

Ten earthworms (*n* = 10) from 3 replicates in each group were chose to conduct the solvent extractions of metabolites. The solvent extraction of the earthworm tissues was described in Brown *et al.*<sup>17</sup> The metabolite extraction strategy used the methanol/chloroform/water system.<sup>18</sup> The main procedures



focused on the following steps. First, the earthworms were starved for two days on moist filter paper in Petri dishes to allow elimination of the gut contents, then the treated earthworms were snap-frozen in liquid nitrogen, lyophilized, weighed and stored at  $-80^{\circ}\text{C}$  in a freezer until required for further analysis. The weights of the lyophilized earthworms ranged from 0.08–0.12 g. Subsequently, the lyophilized earthworms were quickly cut into pieces, samples were extracted using a two-step extraction protocol.<sup>19</sup> First, ice-cold solvent (methanol : water = 4 : 0.85, v/v) was added to the tissue and vortexed for approximately 15 s. Second, ice-cold chloroform (4 mL g<sup>-1</sup> dry earthworm) and water (2 mL g<sup>-1</sup> dry earthworm) were added and vortexed for 60 s. The mixtures were placed into an ice bath for 10 min. Then, the earthworms were homogenized in an ice bath in a 5 mL centrifuge tube using a portable tissue homogenizer with a 6 mm stainless steel spatula (portable tissue homogenizer, S10, Ningbo, China). The samples were kept on ice for 10 min to permit partitioning between the polar and non-polar layers,<sup>9</sup> after which the homogenates were centrifuged at 12 000 rpm for 10 min at  $4^{\circ}\text{C}$ . Next, each supernatant was transferred into a 2 mL centrifuge tube and the organic phase was eliminated under a continuous stream of nitrogen. Then the samples were dissolved in 750  $\mu\text{L}$  of 99.9% D<sub>2</sub>O phosphate buffer (0.2 M, pH 7.4) containing 0.1% (w/v) sodium azide (99.5% purity; Sigma-Aldrich) as a preservative and 0.05% (w/v) sodium 3-(trimethylsilyl)propionate-2,2,3,3-d<sub>4</sub> (TSP, Sigma Aldrich) as an internal standard ( $\delta$  0.0). The samples were then vortexed and centrifuged at 12 000 rpm for 10 min. Finally, each supernatant was transferred into a 5 mm NMR tube for <sup>1</sup>H NMR analysis.

## 2.6 NMR spectroscopy of the earthworm metabolites

<sup>1</sup>H NMR spectra of earthworm extraction were examined using a Bruker AVANCE 500 MHz spectrometer at 298 K (Bruker Bio-spin, Karlsruhe, Germany). A transverse relaxation-edited Carr-Purcell-Meiboom-Gill (CPMG) sequence (90( $\tau$ -180- $\tau$ ),<sub>n</sub>-acquisition) with a total spin-echo delay ( $2n\tau$ ) of 40 ms was used to suppress the signals of macromolecules and proteins. The <sup>1</sup>H NMR spectra were measured using 128 scans into 32k data points over a spectral width of 10 000 Hz. Prior to Fourier transformation, an exponential window function with a line broadening of 0.5 Hz was used for the free induction decays (FIDs).

## 2.7 Spectral data processing

All <sup>1</sup>H NMR spectra were adjusted for phase and baseline using Topspin 3.0 (Bruker GmbH, Karlsruhe, Germany). The ASCII files were subsequently imported into "R".<sup>20</sup> The one-dimensional (1D) spectra were converted to an appropriate format for statistical analysis by automatically segmenting each spectrum into 0.015 ppm integrated spectral regions (buckets) between 0.4 and 9.4 ppm. Regions  $\delta$  4.70–5.25 ppm were deleted to remove any spurious effects of water resonance. Treated spectra were then mean-centered and Pareto-scaled, and the integral values were probability quotient normalized before multivariate statistical analysis.<sup>21</sup>

## 2.8 Data statistical analysis

Metabolites of the earthworm polar extracts in the <sup>1</sup>H NMR spectra were identified by published ref. 9, 17, 22 and 23 with Chenomx NMR Suite 7.7 software (Chenomx Inc., Edmonton, Canada) by querying Human Metabolome Database (HMDB, <http://www.hmdb.ca>). Orthogonal signal correction-partial least squares-discriminant analysis (OSC-PLS-DA) which can decrease the within class variability and confounders that are unrelated to class discrimination were conducted using in-house R scripts (revised PLS packages) to separate the control, Pb1 and Pb2 groups on the 1<sup>st</sup>, 7<sup>th</sup>, 14<sup>th</sup>, 21<sup>st</sup> and 28<sup>th</sup> days. The quality of the OSC-PLS-DA model was evaluated using the repeated two-fold cross-validation (2CV).<sup>24</sup> Cross-validation was evaluated using the parameter  $R^2Y$  and  $Q^2Y$  which were used to avoid overfitting and reflect the predictability of the model. Typically, a  $Q^2Y > 0.4$  is considered a strong model.<sup>8,24</sup> The 2000-times permutation testing was also performed to validate the supervised model. The observed statistical *p*-values (*p* < 0.05) confirmed the significance at a 95% confidence level. The performance measures were plotted as histograms. Metabolites that changed significantly were identified using the color-coded loading plots. The warmer colors show larger more contributions to the class differentiation than the colder colors. The fold change of the metabolites and the associated *p*-values corrected by the Benjamini & Hochberg adjusted method were calculated for multiple comparisons and visualized in a colored table.<sup>25</sup> Parametric (Student's *t* test) tests were conducted to determine the significance of metabolites that were higher or lower between groups and *p* < 0.05 was considered statistically significant. In addition, ANCOVA analysis and PLS regression were conducted using IBM SPSS Statistics 20 and R software.

## 3. Results

### 3.1 Pb concentrations in the earthworms

During the exposure experiment, the survival rates in the various groups ranged from 100% to 90% with increasing time. The mortality rate of earthworms in each group which was less than 10% met the OECD standard. The survival rate of Pb-treated groups decreased to 90% on the 14<sup>th</sup> day, whereas that of the control group reached to 90% on the 21<sup>st</sup> day (Fig. 1A). During the 28 days of exposure, the mean weights of the earthworms in the Pb treated groups obviously deceased after the 14<sup>th</sup> day, whereas those in the control group maintained a relatively constant weight (Fig. 1B). According to the results of the ANCOVA analysis, both time and groups influenced the weight of earthworms, and effects of the groups was larger than that of time (Table S2†).

The Pb concentrations of the earthworms in the Pb-treated groups increased gradually with longer exposure times, and they were much greater in the Pb2 group than that in Pb1 group. In contrast, the Pb concentrations of the earthworms in the CON, which were below 1.5 mg kg<sup>-1</sup>, did not change significantly during the experiment. Specially, the Pb concentrations in the Pb1 group from the 1<sup>st</sup> to the 28<sup>th</sup> day increased from 0.97 to 51.10 mg kg<sup>-1</sup>, whereas those in the Pb2 group were greater, increasing from 1.86 to 91.79 mg kg<sup>-1</sup> (Fig. 2).



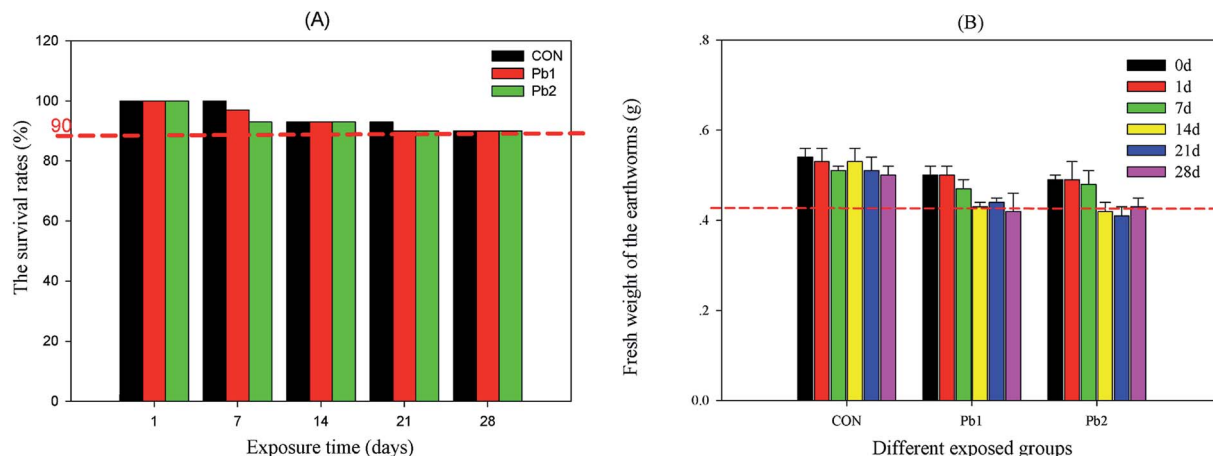


Fig. 1 The survival rate and mean weights of the earthworms during the experiment. CON represents the control group.

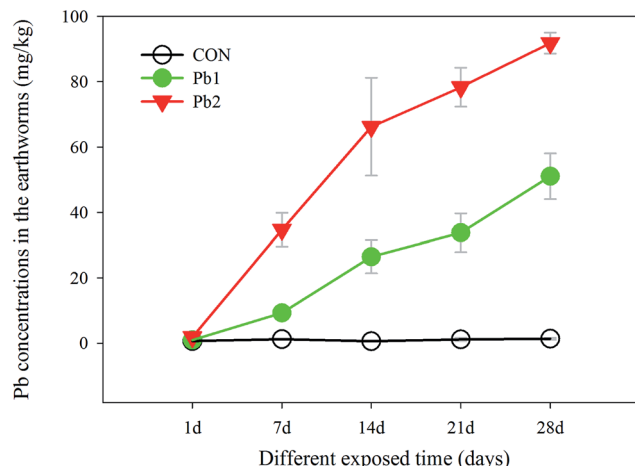


Fig. 2 Changes in the Pb concentrations in the earthworms in the control (CON), Pb1 and Pb2 exposure groups with time.

### 3.2 Histological examinations of the earthworms

The intestinal tissues of the earthworms were intact in the CON group from the 1<sup>st</sup> day to the 28<sup>th</sup> day (Fig. 3), whereas some tissues in Pb1 and Pb2 groups showed slight or severe damages during the experiment. More specifically, on the 1<sup>st</sup> day, the intestinal muscle tissues, circular muscle (CM) and longitudinal muscle (LM), showed the telangiectasia and were filled with red blood cells and the intestinal epithelium (IE) showed slight vesicular degeneration, cytoplasmic vacuoles and a visible oval cavity (plot 2 and 3). Seven days later, the IE demonstrated local necrosis and small circular cavities and had no cell structure, and some earthworms had shed chloragogenous tissues (CT, plot 5 and 6). Two weeks later, the typhlosole (Ty) showed focal necrosis and the LM was separated from the CM, and there were larger irregular cavities in the IE (plot 8). More severe damage was observed in the Pb2 group on the 14<sup>th</sup> day (plot 9). The entire CM and LM showed telangiectasia and were filled with a large number of red blood cells. Most of the CT was separated from the intestinal muscle

tissues. Furthermore, additional large vacuoles appeared in the IE and the overall outline of the intestinal tract was insufficiently clear. On the 21<sup>st</sup> day, small focal necrotic regions appeared in the IE (plot 11 and 12) and the CT was partially separated from the intestinal muscle tissues. At the end of the exposure, the IE demonstrated small areas of local necrosis and some shed CT in Pb1 group (plot 14). The IE in Pb2 group was partially separated from the intestinal muscle tissues, and some CTs became thin. The transition between the CM and LM in Pb2 group was filled with red blood cells (plot 15).

### 3.3 <sup>1</sup>H NMR metabolic profile analysis of earthworms

The <sup>1</sup>H NMR spectra of the earthworm extract samples were investigated and are shown in Fig. S2.† A total 43 metabolites were identified and the details of these metabolites are given in Table S3.† The identified metabolites included primarily compounds involved in energy, amino acid, membrane metabolism.

### 3.4 Multivariate statistical analysis of NMR spectra data

**3.4.1 General analysis of the three exposed groups.** In the OSC-PLS-DA score plot, Pb exposed groups on the 1<sup>st</sup>, 7<sup>th</sup>, 14<sup>th</sup>, 21<sup>st</sup> and 28<sup>th</sup> days were well separated from the control group (Fig. 4A<sup>1</sup>-E<sup>1</sup>). The *p* values of the permutation tests and *R*<sup>2</sup> and *Q*<sup>2</sup> of the 2CV on the 1<sup>st</sup>, 7<sup>th</sup>, 14<sup>th</sup>, 21<sup>st</sup> and 28<sup>th</sup> days were used to confirm the reliability to the grouping in the models and are shown in Fig. 4A<sup>2,3</sup>-E<sup>2,3</sup>. In addition, the OSC-PLS-DA score plots of Pb1- and Pb2-treated groups partially overlapped on the 7<sup>th</sup>, 14<sup>th</sup>, 21<sup>st</sup> and 28<sup>th</sup> days.

The OSC-PLS-DA score plots of the metabolic profiles in Pb1 and Pb2 groups had a distinct time-dependent trajectory relative to the control group (Fig. 5), and the trajectory of the Pb1 and Pb2 groups demonstrated the similar patterns of changing trends but differed in the magnitudes. Components 1 and 2 explained 18.4 and 14.3% of the OSC-PLS-DA, respectively. The data analysis of coordinates mainly focused on the changes in the horizontal direction. The results showed that the coordinates for the 7<sup>th</sup> and 14<sup>th</sup> days were located in the



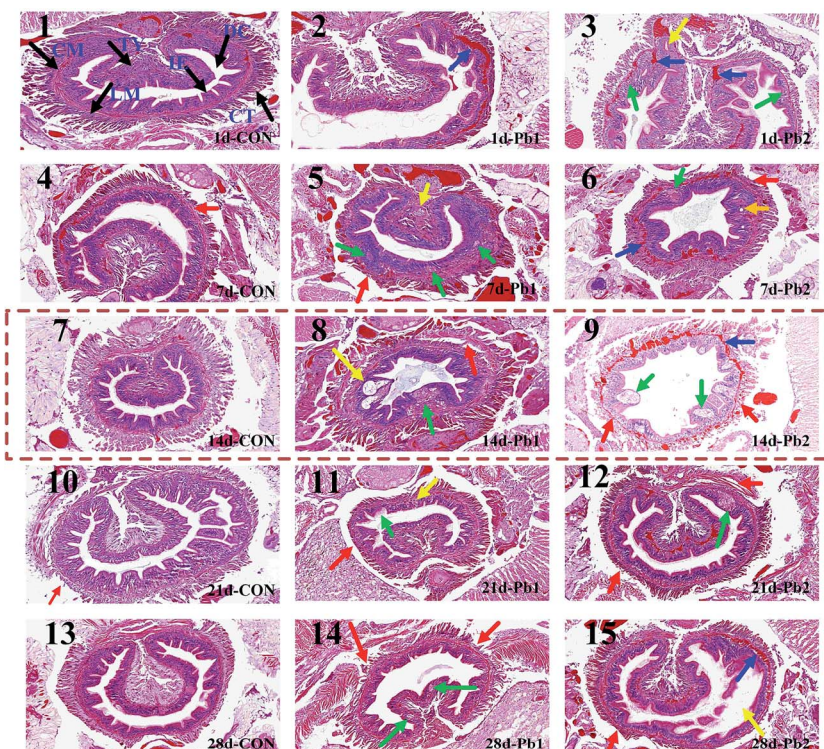


**Fig. 3** The histological examinations of the earthworms with time in the control (CON) and Pb1 and Pb2 groups (plot 1–15,  $\times 200$ ). Panel 1 shows the basic intestinal tissues of the earthworms that are indicated using black arrows including the intestinal epithelium (IE), chloragogenous tissue (CT), circular muscle (CM) and the longitudinal muscle (LM), typhlosole (TY) and digestive cavity (DC). The blue arrows indicated the damage to the transition zone between the LM and CM. The green and yellow arrows indicate for the damage to the IE and TY, which includes slight vesicular degeneration, cell swelling, local necrosis, small or irregular circular cavities, cytoplasmic vacuoles, focal necrosis and the visible oval cavity. The red arrows indicate the damage to the CT including the shedding and becoming thin.

opposite direction to the 1<sup>st</sup> day, and the opposite horizontal distance on the 14<sup>th</sup> day was longer than that on the 7<sup>th</sup> day. After that, the coordinates on the 21<sup>st</sup> and 28<sup>th</sup> days moved toward the positive direction of the coordinate relative to the 1<sup>st</sup> day. The horizontal distance between on the 1<sup>st</sup> and 21<sup>st</sup> day was shorter than that between the 1<sup>st</sup> and 14<sup>th</sup> days. The coordinates on the 28<sup>th</sup> day were located in the positive direction relative to those on the 1<sup>st</sup> day and had a positive distance. Furthermore, compared to the coordinates for the other time points, the maximum distance between the coordinate for the Pb-treated and control groups was reached on the 14<sup>th</sup> day.

**3.4.2 Analysis of each two exposed groups.** The OSC-PLS-DA score plots for the 1<sup>st</sup> day among the Pb1-CON, Pb2-CON and Pb1-Pb2 groups were well separation (Fig. 6). The corresponding *s*-plot and the color-coded loading plots were used to identify potential biomarkers<sup>26</sup> and the contributions of the variables to the grouping of models. The crucial biomarkers, shown in red font, are marked with small rectangular boxes in each *s*-plot. For the comparisons of Pb1-CON and Pb2-CON, the *p* values for the permutation tests were 0.007 and 0.004. Similarly, the  $R^2$  and  $Q^2$  for the model parameters were 0.97–0.80 and 0.98–0.88, respectively (Fig. S3†). In addition, the score plots, *s*-plot and loading plots for the various groups (CON-Pb1, CON-Pb2 and Pb1-Pb2) on the 7<sup>th</sup>, 14<sup>th</sup>, 21<sup>st</sup> and 28<sup>th</sup> days are presented in the ESI (Fig. S4–S7†). The *p* value for the

permutation tests and  $R^2$  and  $Q^2$  of the model parameters for the Pb1-CON, Pb2-CON and Pb1-Pb2 comparisons are also shown in Fig. S3.† Comparing to the control group, the levels of the metabolites involving in alanine, glycerophosphocholine increased in Pb contaminated soils (Pb1 and Pb2) on the 1<sup>st</sup> day, whereas decreases in tyrosine, histidine, myo-inositol, glycine, pyruvate and fumarate were observed (Fig. 7). Metabolites for which significantly differences between the Pb-treated and control groups were observed on the 7<sup>th</sup>, 14<sup>th</sup>, 21<sup>st</sup> and 28<sup>th</sup> days are shown in Fig. 7.

### 3.5 The changing trend for key metabolites with time

According to the peak area of the metabolite in the NMR spectrum which can stand for the relative value of different metabolites, we made the plots of key metabolites against time (Fig. 7). As the exposure time increased, the earthworm metabolites including HEFS, malate and  $\tau$ -methylhistidine first increased on days 1–14 and then decreased on days 14–28. In contrast, metabolites that first decreased and then increased included myo-inositol, scyllo-inositol, betaine, glycerophosphocholine, fumarate and acetylcholine. The minimum values for these compounds occurred on days 7 or 14. In addition, succinate, pyruvate, glutamine and glutamate increase steadily throughout days 1–28. Furthermore, tyrosine, phenylalanine, isoleucine, leucine, valine, lysine, histidine, and

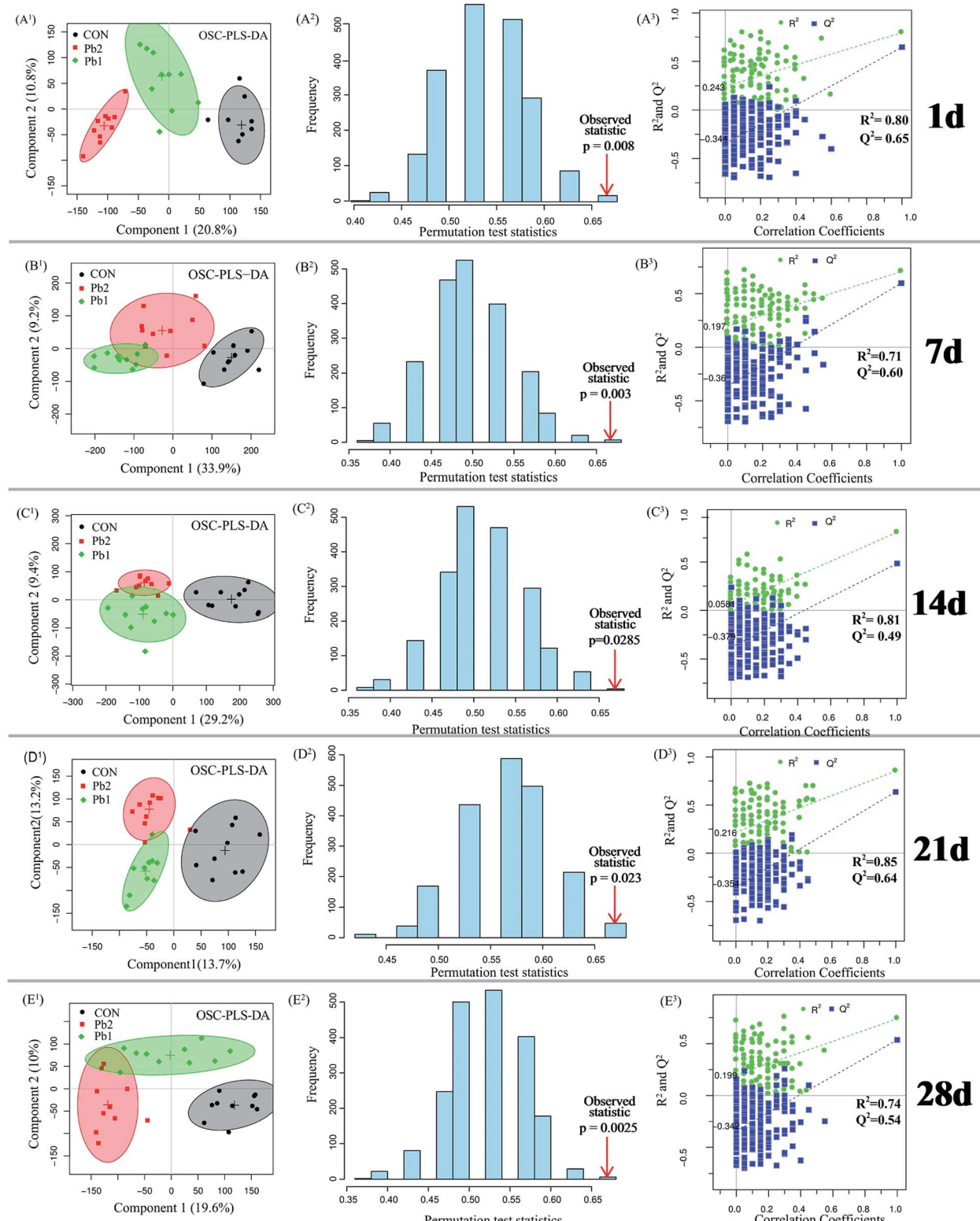


**Fig. 4** The score plots for the OSC-PLS-DA, permutation tests and  $R^2$  and  $Q^2$  for the earthworm extracts from the Pb2, Pb1 and control groups on the 1<sup>st</sup>, 7<sup>th</sup>, 14<sup>th</sup>, 21<sup>st</sup> and 28<sup>th</sup> days. Histograms for the permutation test scores of the OSC-PLS-DA models on the basis of 2000 permutations: the red arrows indicate the performance based on the original labels, which were significant on the basis of demonstrating a  $p$ -value less than 0.05. OSC-PLS-DA scatter plot of the statistical validations obtained from 2000 times permutation tests, with  $R^2$  and  $Q^2$  values in the vertical axis, the correlation coefficients (between the permuted and true class) in the horizontal axis, and the ordinary least squares (OLS) line for the regression of  $R^2$  and  $Q^2$  on the correlation coefficients.

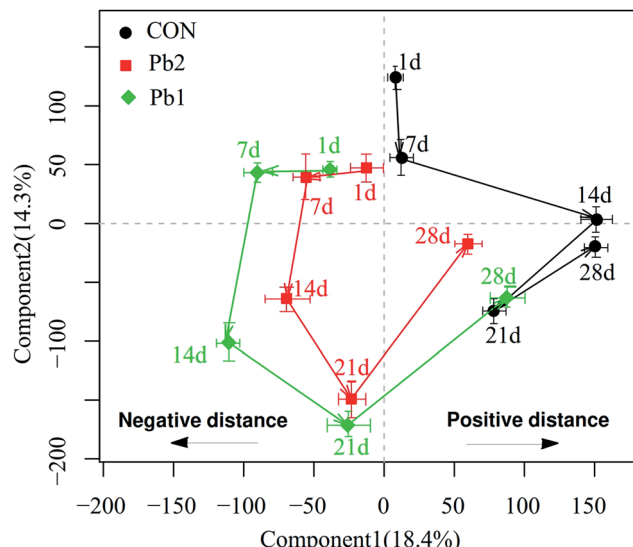


Fig. 5 The OSC-PLS-DA trajectory plot of PC1 (the first OSC-PLS component) and PC2 (the second OSC-PLS component) for mean  $^1\text{H}$  NMR spectra of the polar fraction of the earthworms extracts from the various exposed groups. The designations of 1d, 7d, 14d, 21d and 28d in the plot represent the mean score after days 1, 7, 14, 21 and 28, respectively. The time-response trajectories are shown by the solid lines. Negative and positive distances are relative to the coordinates on the 1<sup>st</sup> day.

choline decreased during days 1–14 and remained relatively stable during days 14–28. The level of maltose, glucose and alanine decreased on days 1–7 and 21–28 and increased on days 7–14.

## 4. Discussion

Evaluations of the metabolic trajectory, histopathological detection, and Pb concentrations as well as the mean weight and survival rates of earthworms were employed to characterize the time-dependent metabolic response of earthworms exposed to L-Pb-CS. The results showed that earthworms may initiate a self-detoxification mechanism after coping with resistance to the L-Pb-CS, and the 14<sup>th</sup> day was the turning point.

### 4.1 The consistency of metabolic trajectory and histopathological analysis

Trajectory plots describe the systemic responses of organisms to physiological perturbations as functions of time.<sup>27</sup> In the present study, the metabolic trajectories for the Pb1 and Pb2 groups demonstrated the similar geometry and patterns, which suggested that the metabolic responses might be of the same type (a similar MOA for earthworms).<sup>27,28</sup> This view was also supported by the same metabolite changes in Pb1 and Pb2 as functions of time, on the basis that they either increased or decreased at the same time rather than demonstrating opposite changes.

As the toxic processes develop through time during the onset, maximal damage and recovery phases, dynamic variation in the metabolic responses to damage appear.<sup>27</sup> The response trajectories as a whole reflected the changing metabolites, and the histopathological analysis directly indicated the organismal damage. The distance of the coordinates of the trajectory from the corresponding initial coordinate could be linked to the phase of the organismal lesion.<sup>29</sup> We assumed that the negative

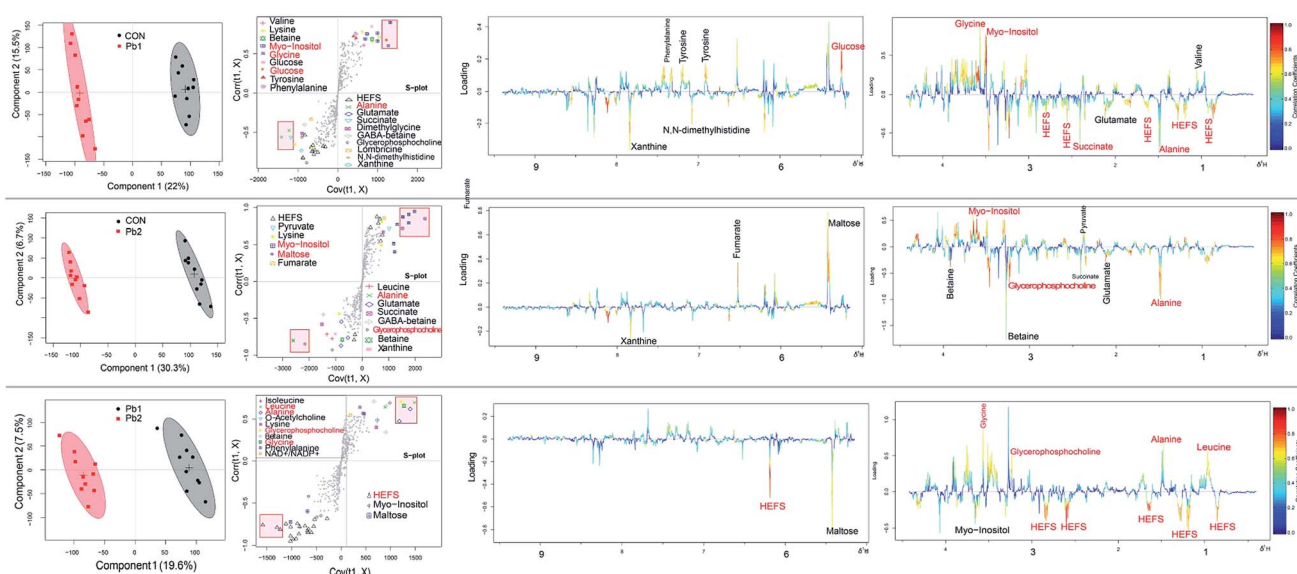


Fig. 6 The score plots, s-plot and loading plots in different groups (CON–Pb1, CON–Pb2 and Pb1–Pb2) on the 1<sup>st</sup> day. Score plot where one point represented one sample and one ellipse corresponded to a confidence interval of 95% stood for a grouping. The s-plot where points represented different variables (metabolites). The crucial biomarker in red font were marked with a small rectangular box in each s-plot. Loading plots (0.4–4.42 and 5.15–9.4 ppm) color coded according to the correlation coefficients from blue to red. The color bar corresponds to the weight of the corresponding variable in the discrimination of statistically significant (red) or no significant (blue). Positive and negative peaks indicated a relatively decreased and increased metabolite level in the Pb (Pb1 or Pb2) exposed groups.



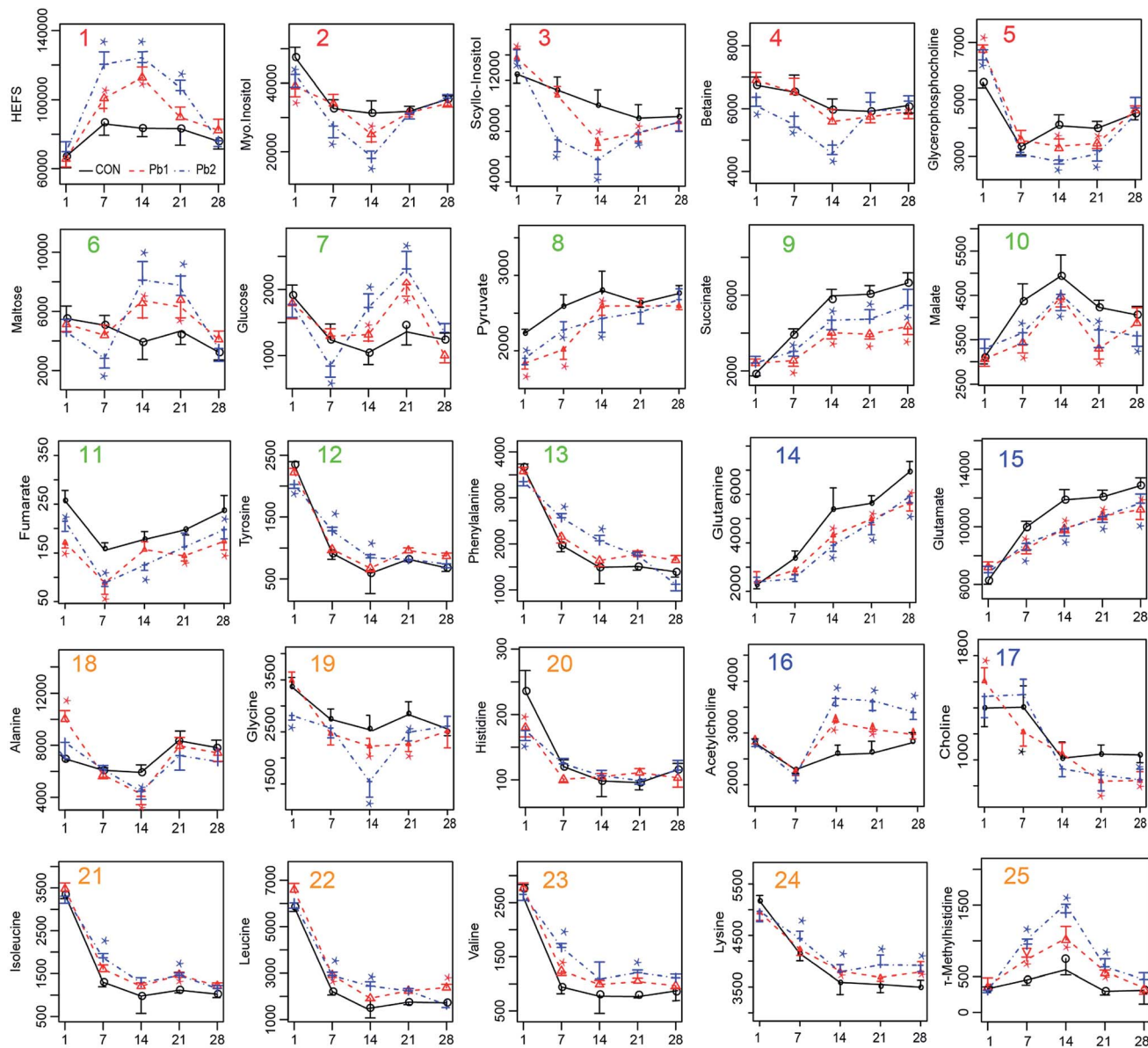


Fig. 7 Plots of the key metabolites metabolite concentration against time. The changes of the metabolites in the CON, Pb1 and Pb2 groups are expressed in three different colors: black, red and blue, respectively. The Y axis represents the peak area of the metabolite. The blue and red marker “\*” indicates significant differences ( $p < 0.05$ ) in the metabolites between control and Pb2 and between control and Pb1, respectively.

motion relative to the coordinate on the 1<sup>st</sup> day in the trajectory plot represented an adverse effect and that the positive movement represented an adaptation to the adverse effects. The coordinates of the Pb treated groups on the 7<sup>th</sup> and 14<sup>th</sup> days moved in negative direction and the negative horizontal distance increased gradually relative to the 1<sup>st</sup> day. This suggested that during the initial 14 days, the earthworms that were exposed to in L-Pb-CS showed a toxic response to the stress. In contrast, after 14 days of exposure, the coordinates moved in the positive direction and closely approached the coordinate of the control group on the 28<sup>th</sup> day while the positive horizontal distance gradually increased. Earthworms may produce a detoxification mechanism after 14 days to adapt to the L-Pb-CS but full biochemical recovery from the toxic damage had

not occurred by the 28<sup>th</sup> day. According to the OSC-PLS-DA score plot, the dose effect in various groups on the 1<sup>st</sup> and 28<sup>th</sup> days can be interpreted as initial toxic effects and late metabolic recovery, respectively, whereas the overlaps between the Pb1- and Pb2-treated groups at the other times can be explained as the overall influence of a metabolic disorder due to the Pb toxic effects. A parallel type of response trajectories has also been reported for male fish exposed to the estrogen 17 $\alpha$ -ethynodiol<sup>11</sup> and for rats exposed to various doses of mercury(II) chloride and 2-bromoethanamine.<sup>30</sup> In addition, the coordinates of the Pb-treated groups reached a maximum negatively horizontal distance between on the 14<sup>th</sup> and 1<sup>st</sup> days, and the difference in the distance between the coordinates for the Pb-treated and control groups on the 14<sup>th</sup> day was also greater

than that at the other time points. Histological analyses were used to identify pathology and evidence of inflammation in the tissue.<sup>31</sup> Histopathological detection of the Pb-treated groups, especially Pb2 group, on the 14<sup>th</sup> day indicated that the IE demonstrated large vacuolization, cellular edema and severe necrosis. To some extent, the most serious damage during the exposure time occurred on the 14<sup>th</sup> day. In other words, the MOA in earthworms between days 1–14 and days 14–28 may differ, and histopathological analysis and metabolic trajectory could provide mutually supportive data. Therefore, the applicable exposure time for earthworm toxicological metabolomics should be considered in real heavy metal contaminated soils. We recommend 14 days of exposure, which is consistent with the exposure time for the acute toxicity test of earthworms.<sup>7</sup>

#### 4.2 Metabolite responses and metabolic process

Weight change can be an excellent indicator of environmental stress because some metabolic responses may ultimately be linked to weight reduction.<sup>32</sup> Because cattle manure was added to the exposed soils as the food for the earthworms, the decrease in the mean weights was considered to be the result of the L-Pb-CS stress and exposure time rather than food deficiency, which was consistent with the ANCOVA analysis (Table S2†). The survival rates of the earthworms in this study were also associated with the soil Pb concentrations and the exposure times. The times required to decrease the survival rates to less than 90% were Pb2 < Pb1 < CON. The Pb concentrations in the earthworms were much lower than those in the soil, and the bioaccumulation factor was much less than one, which suggested that the Pb binding with soils did not accumulate but instead concentrated in the earthworms. Furthermore, increasing Pb concentrations in the earthworms from the L-Pb-CS caused different metabolic responses. The time-dependent exposure to L-Pb-CS mainly disturbed the amino acid, membrane and energy metabolism in the earthworms.

#### 4.3 Amino acids mechanism

The cell stress response (CSR) that is characteristic of all cells is a defense reaction to a strain imposed by environmental force. Such strain commonly causes deformation or damage to proteins, DNA, or other essential macromolecules.<sup>33</sup> Previous studies show that Pb can cause the overproduction of intracellular reactive oxygen species (ROS).<sup>34,35</sup> In this study, the histopathological evaluation also showed various degrees of tissue damages and necrosis in Pb-treated groups throughout the whole exposure process. In addition, the cellular levels of both alanine and glycine are known to exert a cytoprotective action against stress damage by contaminants<sup>36</sup> and can induce the gene expression and synthesis of stress protein.<sup>37,38</sup> Earthworms may cope with the oxidative damage to the intestine caused by the L-Pb-CS, which resulted in the continuous consumption of alanine and glycine on days 1–14 and reached the minimum values on the 14<sup>th</sup> day. Furthermore, there are more consumption in Pb-treated groups in contrast to the control group. Exposure medium to the low Pb-contaminated soil may induce a detoxification strategy in the earthworm<sup>39</sup> before death such

that the levels of these amino acids gradually increased on days 14–28. Furthermore, the level of isoleucine, leucine and valine (branched-chain amino acids, BCAA) as well as lysine decreased on days 1–14 and remained relatively stable on days 14–28. The results for the BCAA on days 1–14 are consistent with the results of exposure of earthworms to phenanthrene.<sup>40</sup> The decrease and steady state in amino acids with time changing may be linked to weight loss of earthworms due to the stress of the L-Pb-CS. Studies show that BCAA levels decrease with weight loss.<sup>41,42</sup> The level of  $\tau$ -methylhistidine which represents the breakdown of muscle protein,<sup>43</sup> increased on days 1–14 and decreased on days 14–28, which suggested that protein degradation may have occurred. However, the damage to the tissues was simultaneously accompanied by repair that involved amino acids synthesis. In general, the levels of amino acids in Pb treated groups were higher compared with that in control group. Therefore, the amino acids whose concentrations decreased may have been used to synthesize proteins to repair the damaged tissues as the result of the activation of a detoxification strategy.<sup>44</sup> These results suggested that the metabolic response to L-Pb-CS exposure differed between days 1–14 and days 14–28. Further evaluation of the metabolic response to long-term exposure to L-Pb-CS along with other omics approaches may help to interpret the phenomenon.<sup>3</sup>

#### 4.4 Osmotic equilibrium

Myo-inositol, scyllo-inositol, betaine and glycerophosphocholine are common organic osmolytes in biological systems that assist in maintaining the osmotic balance in cells.<sup>45,46</sup> HEFS is a compound unique to earthworms that is found in numerous species such as *Lumbricus rubellus* and *E. fetida*.<sup>47,48</sup> Furthermore, HEFS which may be a gut surfactants,<sup>49</sup> plays a vital role in membrane stabilization due to its amphiphilic property.<sup>3</sup> Pb contaminated soils were ingested and transferred to the earthworm intestine. Under the specific intestinal conditions, some Pb<sup>2+</sup> in the soil likely entered into the IE via the Ca<sup>2+</sup> channel.<sup>50</sup> A large amount of Ca<sup>2+</sup> was released to the cytoplasm after a series of induced reactions.<sup>51</sup> The process can cause an osmotic imbalance (edema and vacuolization of the IE) of some cells due to abnormal Ca<sup>2+</sup> concentration inside and outside the membrane.<sup>52</sup> Distinct profiles of the changes in the various osmolytes that serve to maintain the membrane stability were observed during the exposure process,<sup>53,54</sup> especially on the 14<sup>th</sup> day. The levels of HEFS increased on days 1–14 and reached to a peak value on the 14<sup>th</sup> day, subsequently decreased gradually on days 14–28 and close to the level of the first day, whereas myo-inositol, scyllo-inositol, betaine and glycerophosphocholine continuously decreased or reached to a minimum value on the 14<sup>th</sup> day and then increased gradually until the 28<sup>th</sup> day. Previous studies in terms of polycyclic aromatic hydrocarbons and endosulfan also presented the disturbance of betaine and myo-inositol of earthworms.<sup>28,53</sup> Furthermore, changes of osmolytes are often associated with edema and deformity of cells.<sup>55</sup> It is likely that osmolytes uptake is in excess of osmolytes loss due to the stress of the L-Pb-CS. Thereafter, an osmotic force may be created, which will cause the net increase



of cellular water with the latter the pathological equivalent of cell edema.<sup>56</sup> Some of the IE in the Pb1 and Pb2 groups demonstrated cell edema and cytoplasmic vacuoles on the 14<sup>th</sup> day based on the histological detection. The changes in various osmolytes suggested that the osmotic balance in the earthworms may have been disturbed<sup>53</sup> by the L-Pb-CS with the maximum change occurring on the 14<sup>th</sup> day. A gradual recovery was then observed until the 28<sup>th</sup> day (without reaching the initial or control level).

#### 4.5 Energy metabolism

During the exposures, the energy expenditure of the earthworms improved due to the stress of L-Pb-CS. Maltose which is an intermediate formed by the breakdown of glycogen and starches during digestion<sup>57</sup> can be broken down into two glucose molecules by hydrolysis in living organisms to produce energy.<sup>43</sup> Then the breakdown of glucose to pyruvate by glycolysis is linked to the citric acid cycle (CAC), which is the main energy transfer cycle for energy production in living organisms.<sup>43</sup> The earthworms rapidly take advantage of maltose and glucose from food digestion following decreases in these compounds in the first 7 days of exposure due to the gut purge before exposure so that they can maintain normal metabolic changes. As the stress due to the L-Pb-CS and the Pb concentration in the earthworms increased, the earthworms may need more energy to fight toxicity, which resulted in a sharp increase in these compounds on the 14<sup>th</sup> and 21<sup>st</sup> days.<sup>53</sup> Moreover, the peak value of glucose was delayed relative to that of maltose. The changes of maltose and glucose may be related to the detoxification strategy of earthworms.<sup>58</sup> Succinate, fumarate and malate are part of the Krebs cycle, which is an integral pathway in energy metabolism.<sup>43</sup> The levels of succinate continuously increased throughout the experiment. The level of fumarate gradually increased and reached a maximum value on the 7<sup>th</sup> day and then decreased during the subsequent exposure period. However, the level of malate showed an opposite trend of change and reached a maximum value on the 14<sup>th</sup> day. Furthermore, the levels in Pb-treated groups was also lower than that of control group, which suggested that their consumption was greater in the Pb-treated groups due to the L-Pb-CS-induced stress.<sup>53</sup> These results clearly suggested a dynamic disturbance of energy metabolism in earthworms. Previous studies show that copper and phenanthrene exposure also caused a disruption in energy metabolism of earthworms.<sup>3,59</sup>

In general, L-Pb-CS may cause neurotoxic effects, disorders in energy mechanism, osmotic equilibrium and amino acids mechanism in earthworms. Detecting the changes in the level of metabolites in response to environmental stressors can identify possible biomarkers for the stressor.<sup>3,11</sup> Among the changing metabolites, the crucial ones shown in red font of each loading plots which are important metabolites contributing to the separation<sup>60</sup> between control *E. fetida* and those exposed to Pb treated groups are also marked with small rectangular boxes in each s-plot from the 1<sup>st</sup> to the 28<sup>th</sup> day. Furthermore, we counted the number of markers in the various

groups throughout the experiment (Fig. S8†). Myo-inositol, HEFS, scyllo-inositol, succinate, alanine and maltose which were ranked in the top 6 key metabolites were most likely used as potential biomarkers for the actual Pb contamination in the soil. Other reports show that alanine is considered as the universal stress signal and may be of use as a potential biomarker.<sup>37,53,61</sup> Maltose is also identified as potential indicators of phenanthrene and mixture metal exposure.<sup>9,53,62</sup> When the use of PLS regression analysis to explore the relationship between Pb concentrations and metabolites of the earthworms showed that there is a strong correlation between lead content and the levels of HEFS, myo-inositol and scyllo-inositol (Fig. S9†). Therefore, these three special metabolites of earthworm should be helpful as biomarkers for the detection of low lead contaminated soils in the future.

Although earthworms may initiate a detoxification strategy to address the L-Pb-CS stress, it cannot be concluded that L-Pb-CS is safe for soil organisms. We conducted only a four-week exposure experiment, in which Pb concentrations in the earthworms reached approximately 100 mg kg<sup>-1</sup> and there could be a further increasing trend with longer periods of exposure. Chronic exposure to the same levels of contaminants in the soil may have more detrimental consequences of earthworms than short-term exposure.<sup>39</sup> A previous study indicated that long-term conditions of low Pb concentrations in the blood of children not only caused neurotoxicity but also affected the intellectual development.<sup>63</sup> Longer exposure of earthworms to L-Pb-CS may have some unexpected slow toxicity. Therefore, genomics, transcriptomics and proteomics should also be implemented to identify the upstream regulatory genes and response proteins associated with the changing metabolites to better explain the MOA of L-Pb-CS in earthworms if condition permits in the future.

## 5. Conclusion

In this study the value of a metabolomics approach coupled with histological analysis and basic phenotypic endpoints (survival, weight change) for assessing the time-metabolic response to the exposure of *E. fetida* earthworm to the L-Pb-CS has been clearly presented. We found that the metabolic responses of the earthworms in the Pb-treated groups showed similar mechanisms but differed in the magnitudes of the responses on the basis of the metabolic trajectory and histopathological analyses. The metabolic responses of the earthworms differed between days 1–14 and 14–28. We inferred that earthworms may initiate a detoxification strategy in response to the L-Pb-CS stress. Based on the large changes in the metabolic trajectories and histological results in the earthworms, fourteen days is recommended as the exposure time for earthworm ecotoxicology metabolomics in soils contaminated with low levels of Pb. In addition, the disturbed metabolites were primarily involved in disorder of energy, osmotic equilibrium and amino acid mechanisms in the earthworms. Myo-inositol, HEFS, scyllo-inositol, succinate, alanine and maltose could be used as potential biomarkers for the soils contaminated with low levels of Pb. This method is expected to have a potential



monitoring application for real world soils contaminated with heavy metals by characterizing the metabolic responses of earthworms in contaminated habitats.

## Conflicts of interest

There are no conflicts of interest to declare.

## Acknowledgements

This research was supported by the National Key Research and Development Plan of China (2016YFD0800400). We thank Minghui Li, School of Environmental and Biological Engineering, Nanjing University of Science and Technology, Shanting Liao, Department of Natural Medicinal Chemistry, China Pharmaceutical University. We are grateful to the anonymous reviewers for their insightful points and suggestions for improvement of this manuscript.

## References

- 1 J. K. Nicholson and J. C. Lindon, *Nature*, 2008, **455**, 1054–1056.
- 2 J. Delaney, E. Clarke, D. Hughes and M. Rice, *Drug Discovery Today*, 2006, **11**, 839–845.
- 3 J. G. Bundy, J. K. Sidhu, F. Rana, D. J. Spurgeon, C. Svendsen, J. F. Wren, S. R. Stürzenbaum, A. J. Morgan and P. Kille, *BMC Biol.*, 2008, **6**, 1.
- 4 J. K. Nicholson, J. C. Lindon and E. Holmes, *Xenobiotica*, 1999, **29**, 1181–1189.
- 5 M. J. Simpson and J. R. McKelvie, *Anal. Bioanal. Chem.*, 2009, **394**, 137–149.
- 6 J. Sanchez-Hernandez, in *Reviews of environmental contamination and toxicology*, Springer, 2006, pp. 85–126.
- 7 OECD, 1984.
- 8 O. A. Jones, D. J. Spurgeon, C. Svendsen and J. L. Griffin, *Chemosphere*, 2008, **71**, 601–609.
- 9 B. P. Lankadurai, D. M. Wolfe, M. L. W. Åslund, A. J. Simpson and M. J. Simpson, *Metabolomics*, 2013, **9**, 44–56.
- 10 J. Yuk, M. J. Simpson and A. J. Simpson, *Environ. Pollut.*, 2013, **175**, 35–44.
- 11 D. Ekman, Q. Teng, D. Villeneuve, M. Kahl, K. Jensen, E. Durhan, G. Ankley and T. Collette, *Environ. Sci. Technol.*, 2008, **42**, 4188–4194.
- 12 D. R. Ekman, Q. Teng, D. L. Villeneuve, M. D. Kahl, K. M. Jensen, E. J. Durhan, G. T. Ankley and T. W. Collette, *Metabolomics*, 2009, **5**, 22.
- 13 M. R. Viant, J. G. Bundy, C. A. Pincetich, J. S. de Ropp and R. S. Tjeerdenma, *Metabolomics*, 2005, **1**, 149–158.
- 14 J. R. McKelvie, J. Yuk, Y. Xu, A. J. Simpson and M. J. Simpson, *Metabolomics*, 2009, **5**, 84–94.
- 15 Ministry of Environmental Protection and Ministry of Land and Resources People's Republic of China, *Bulletin National Survey of Soil Pollution*, 2014, in chinese.
- 16 F.-J. Zhao, Y. Ma, Y.-G. Zhu, Z. Tang and S. P. McGrath, *Environ. Sci. Technol.*, 2014, **49**, 750–759.
- 17 S. A. Brown, A. J. Simpson and M. J. Simpson, *Environ. Toxicol. Chem.*, 2008, **27**, 828–836.
- 18 C. Y. Lin, H. Wu, R. S. Tjeerdenma and M. R. Viant, *Metabolomics*, 2007, **3**, 55–67.
- 19 H. Wu, A. D. Southam, A. Hines and M. R. Viant, *Anal. Biochem.*, 2008, **372**, 204–212.
- 20 R. C. Team, *R: A language and environment for statistical computing*, *R: Foundation for Statistical Computing*, Vienna, Austria, 2013.
- 21 F. Dieterle, A. Ross, G. Schlotterbeck and H. Senn, *Anal. Chem.*, 2006, **78**, 4281–4290.
- 22 S. J. Rochfort, V. Ezernieks and A. L. Yen, *Metabolomics*, 2009, **5**, 95–107.
- 23 M. Liebeke and J. G. Bundy, *Biochem. Biophys. Res. Commun.*, 2013, **430**, 1306–1311.
- 24 J. A. Westerhuis, H. C. Hoefsloot, S. Smit, D. J. Vis, A. K. Smilde, E. J. van Velzen, J. P. van Duijnhoven and F. A. van Dorsten, *Metabolomics*, 2008, **4**, 81–89.
- 25 Y. Benjamini and Y. Hochberg, *J. Roy. Stat. Soc. B*, 1995, 289–300.
- 26 C. Guo, X.-y. Huang, M.-j. Yang, S. Wang, S.-t. Ren, H. Li and X.-x. Peng, *Fish Shellfish Immunol.*, 2014, **39**, 215–222.
- 27 H. C. Keun, T. M. Ebbels, M. E. Bolland, O. Beckonert, H. Antti, E. Holmes, J. C. Lindon and J. K. Nicholson, *Chem. Res. Toxicol.*, 2004, **17**, 579–587.
- 28 J. Yuk, Ph.D thesis, University of Toronto, 2012.
- 29 B. Beckwith-Hall, J. Nicholson, A. Nicholls, P. Foxall, J. Lindon, S. Connor, M. Abdi, J. Connelly and E. Holmes, *Chem. Res. Toxicol.*, 1998, **11**, 260–272.
- 30 E. Holmes, F. Bonner, B. Sweatman, J. Lindon, C. Beddell, E. Rahr and J. Nicholson, *Mol. Pharmacol.*, 1992, **42**, 922–930.
- 31 M. J. Van Der Ploeg, R. D. Handy, L.-H. Heckmann, A. Van Der Hout and N. W. Van Den Brink, *Nanotoxicology*, 2013, **7**, 432–440.
- 32 P. Brown, S. Long, D. Spurgeon, C. Svendsen and P. Hankard, *Chemosphere*, 2004, **57**, 1675–1681.
- 33 D. Kütz, *Annu. Rev. Physiol.*, 2005, **67**, 225–257.
- 34 T. Chen, Y. Liu, M.-H. Li, H.-D. Xu, J.-Y. Sheng, L. Zhang and J.-S. Wang, *Environ. Chem.*, 2016, **13**, 792–803.
- 35 S. Maity, S. Roy, S. Chaudhury and S. Bhattacharya, *Environ. Pollut.*, 2008, **151**, 1–7.
- 36 I. Nissim, M. Hardy, J. Pleasure, I. Nissim and B. States, *Kidney Int.*, 1992, **42**, 775–782.
- 37 M. Forcella, E. Berra, R. Giacchini, B. Rossaro and P. Parenti, *Ecotoxicol. Environ. Saf.*, 2007, **66**, 326–334.
- 38 A. Howard, I. Tahir, S. Javed, S. M. Waring, D. Ford and B. H. Hirst, *J. Physiol.*, 2010, **588**, 995–1009.
- 39 J. Žaltauskaitė and I. Sodienė, *Ecotoxicol. Environ. Saf.*, 2014, **103**, 9–16.
- 40 J. R. McKelvie, D. M. Wolfe, M. Celejewski, A. J. Simpson and M. J. Simpson, *Environ. Pollut.*, 2010, **158**, 2150–2157.
- 41 B. Laferrière, D. Reilly, S. Arias, N. Swerdlow, P. Gorroochurn, B. Bawa, M. Bose, J. Teixeira, R. D. Stevens and B. R. Wenner, *Sci. Transl. Med.*, 2011, **3**, 80re2.



42 S. Shah, D. Crosslin, C. Haynes, S. Nelson, C. Turer, R. Stevens, M. Muehlbauer, B. Wenner, J. Bain and B. Laferrere, *Diabetologia*, 2012, **55**, 321–330.

43 H. R. Horton, L. A. Moran, R. S. Ochs, J. D. Rawn and K. G. Scrimgeour, *Principles of biochemistry*, Prentice Hall Upper Saddle River, NY, 1996.

44 S. R. Stürzenbaum, O. Georgiev, A. J. Morgan and P. Kille, *Environ. Sci. Technol.*, 2004, **38**, 6283–6289.

45 K. Strange, R. Morrison, C. W. Heilig, S. DiPietro and S. R. Gullans, *Am. J. Physiol.: Cell Physiol.*, 1991, **260**, C784–C790.

46 R. D. Bowlus and G. N. Somero, *Science*, 1982, **217**, 1214–1222.

47 J. G. Bundy, H. C. Keun, J. K. Sidhu, D. J. Spurgeon, C. Svendsen, P. Kille and A. J. Morgan, *Environ. Sci. Technol.*, 2007, **41**, 4458–4464.

48 Q. Guo, J. K. Sidhu, T. M. Ebbels, F. Rana, D. J. Spurgeon, C. Svendsen, S. R. Stürzenbaum, P. Kille, A. J. Morgan and J. G. Bundy, *Metabolomics*, 2009, **5**, 72–83.

49 M. Liebeke, N. Strittmatter, S. Fearn, A. J. Morgan, P. Kille, J. Fuchser, D. Wallis, V. Palchykov, J. Robertson and E. Lahive, *Nat. Commun.*, 2015, **6**, 7869.

50 M. Kirberger, H. C. Wong, J. Jiang and J. J. Yang, *J. Inorg. Biochem.*, 2013, **125**, 40–49.

51 F. A. Schanne, G. J. Long and J. F. Rosen, *Biochim. Biophys. Acta, Mol. Basis Dis.*, 1997, **1360**, 247–254.

52 M. A. Verity, *Environ. Health Perspect.*, 1990, **89**, 43.

53 B. P. Lankadurai, D. M. Wolfe, A. J. Simpson and M. J. Simpson, *Environ. Pollut.*, 2011, **159**, 2845–2851.

54 C. R. Petersen, M. Holmstrup, A. Malmendal, M. Bayley and J. Overgaard, *J. Exp. Biol.*, 2008, **211**, 1903–1910.

55 J. Cordoba, J. Gottstein and A. T. Blei, *Hepatology*, 1996, **24**, 919–923.

56 N. A. Tobey, E. J. Cragoe and R. C. Orlando, *Gastroenterology*, 1995, **109**, 414–421.

57 S. A. Jones, M. Jorgensen, F. Z. Chowdhury, R. Rodgers, J. Hartline, M. P. Leatham, C. Struve, K. A. Krogfelt, P. S. Cohen and T. Conway, *Infect. Immun.*, 2008, **76**, 2531–2540.

58 W. Zhang, K. Liu, J. Li, J. Liang and K. Lin, *J. Hazard. Mater.*, 2015, **300**, 737–744.

59 S. A. Brown, J. R. McKelvie, A. J. Simpson and M. J. Simpson, *Environ. Pollut.*, 2010, **158**, 2117–2123.

60 J. R. McKelvie, J. Yuk, Y. Xu, A. J. Simpson and M. J. Simpson, *Metabolomics*, 2009, **5**, 84.

61 S. A. Brown, A. J. Simpson and M. J. Simpson, *Environ. Chem.*, 2009, **6**, 432–440.

62 J. G. Bundy, D. J. Spurgeon, C. Svendsen, P. K. Hankard, J. M. Weeks, D. Osborn, J. C. Lindon and J. K. Nicholson, *Ecotoxicology*, 2004, **13**, 797–806.

63 M. Jakubowski, *International Journal of Occupational Medicine and Environmental Health*, 2011, **24**, 1–7.

